

Modulational instability in nonlocal Kerr-type media with random parameters

E.V. Doktorov* and M.A. Molchan†

B.I. Stepanov Institute of Physics, 68 F. Skaryna Ave., 220072 Minsk, Belarus

Modulational instability of continuous waves in nonlocal focusing and defocusing Kerr media with stochastically varying diffraction (dispersion) and nonlinearity coefficients is studied both analytically and numerically. It is shown that nonlocality with the sign-definite Fourier images of the medium response functions suppresses considerably the growth rate peak and bandwidth of instability caused by stochasticity. Contrary, nonlocality can enhance modulational instability growth for a response function with negative-sign bands.

PACS numbers: 42.25.Dd, 42.70.-a, 42.65.Jx

I. INTRODUCTION

Modulational instability (MI) in nonlinear media is a destabilization mechanism which produces a self-induced breakup of an initially continuous wave into localized (solitary wave) structures. This phenomenon was predicted in plasma [1, 2], nonlinear optics [3, 4], fluids [5] and atomic Bose-Einstein condensates [6, 7, 8]. MI of continuous waves can be used to generate ultra-high repetition-rate trains of soliton-like pulses [9, 10, 11]. It is common knowledge that MI is absent in the defocusing Kerr medium and presents as the long-wave instability with a finite bandwidth in the focusing Kerr medium [12].

The above results were obtained for media with deterministic parameters. Contrary, in realistic media the characteristic parameters are not constants, as a rule, but fluctuate randomly around their mean values. It was shown in the setting of nonlinear optics that stochastic inhomogeneities in a Kerr-type medium extend the domain of MI of continuous waves, as compared with deterministic systems, over the whole spectrum of modulation wavenumbers, even for the defocusing regime [13, 14, 15]. A comprehensive review of MI of electromagnetic waves in inhomogeneous and in discrete media is given in Ref. [16].

Another important aspect of a class of realistic nonlinear media is concerned with their nonlocality. Nonlocality is typically a result of underlying transport processes such as heat conduction in thermal nonlinear media [17], diffusion of atoms in a gas [18], long-range electrostatic interaction in liquid crystals [19], charge carrier transfer in photorefractive crystals [20, 21], and many-body interaction in Bose-Einstein condensates [22]. Nonlocality can prevent the collapse of self-focused beams [23, 24] and dramatically alter interaction between dark solitons [25]. MI in deterministic nonlocal Kerr-type media was studied in Refs. [26, 27], and it was shown that nonlocality does not produce MI in the defocusing case for small and moderate values of the product “modulation amplitude

× nonlocality parameter”.

In the present paper we unite the two above lines of study of nonlinear media and analyze MI in nonlocal media with stochastic parameters. Since nonlocality spreads out localized excitations, it is reasonable to expect a partial suppression of the stochasticity-induced MI gain. Indeed, we demonstrate that the aforementioned situation with MI in local stochastic media with the sign-definite Fourier images of the response functions changes drastically, if nonlocality is taken into account. Namely, both the growth rate peaks and bandwidths of instability are considerably decreased. On the other hand, there can be an “anomalous” behavior of nonlocality when the Fourier image of the response function of a nonlocal medium allows for sign-negative bands. In this case the MI gain of a nonlocal medium can exceed that of a local stochastic medium for some values of the modulation wavenumber. We adopt the nonlocal nonlinear Schrödinger equation with random coefficients as a model to reveal peculiarities of MI of continuous waves. The results obtained are illustrated by the white noise model for parameter fluctuations and by response functions of several types.

II. MODEL

The propagation of an optical beam along the z axis in a nonlocal medium with random parameters is governed by the nonlinear Schrödinger equation

$$iu_z + \frac{1}{2}d(z)u_{xx} + g(z)u \int_{-\infty}^{\infty} dx' R(x-x')|u|^2(x', z) = 0. \quad (2.1)$$

Here x is the transverse coordinate, $u(x, z)$ is the complex envelope amplitude and we use the standard dimensionless variables. The group velocity dispersion (or diffraction) coefficient $d(z)$ and nonlinearity coefficient $g(z)$ are considered as stochastic functions which fluctuate around their mean values d_0 ($d_0 > 0$) and g_0 ($g_0 \geq 0$):

$$d(z) = d_0(1 + m_d(z)), \quad g(z) = g_0(1 + m_g(z)). \quad (2.2)$$

Here m_d and m_g are independent zero-mean random processes of the Gaussian white-noise type,

$$\langle m_d \rangle = \langle m_g \rangle = 0, \quad \langle m_d(z)m_d(z') \rangle = 2\sigma_d^2\delta(z-z'),$$

*Electronic address: doktorov@dragon.bas-net.by

†Electronic address: m.moltschan@dragon.bas-net.by

$$\langle m_g(z)m_g(z') \rangle = 2\sigma_g^2\delta(z-z'),$$

and the angle brackets stand for the expectation with respect to the distribution of the processes $m_d(z)$ and $m_g(z)$. The integral in equation (2.1) represents the field-intensity dependent change of the refractive index characterized by the normalized symmetric response function $R(x)$, $\int_{-\infty}^{\infty} dx R(x) = 1$. The delta-function response function $R(x) = \delta(x)$ corresponds to the local limit of the model. We will discriminate between the focusing ($g_0 > 0$) and defocusing ($g_0 < 0$) media.

Eq. (2.1) possesses the homogeneous plane wave solution

$$u_0 = A \exp \left[iA^2 \int_0^z dz' g(z') \right], \quad (2.3)$$

where A is a real amplitude. Now we perform the linear stability analysis of the solution (2.3). Assume that

$$u(x, z) = (A + v(x, z)) \exp \left[iA^2 \int_0^z dz' g(z') \right] \quad (2.4)$$

is a perturbed solution of Eq. (2.1) with $v(x, z)$ being a small complex modulation. Substituting Eq. (2.4) into Eq. (2.1) and linearizing about the plane wave (2.3), we get a linear equation for $v(x, z)$:

$$iv_z + \frac{1}{2}d(z)v_{xx} + 2g(z)A^2 \int dx' R(x-x') \text{Re} v(x', z) = 0. \quad (2.5)$$

After decomposing v into real and imaginary parts, $v = r(x, z) + is(x, z)$, and performing the Fourier transforms

$$\rho(k, z) = \frac{1}{2\pi} \int_{-\infty}^{\infty} dx r(x, z) e^{ikx},$$

$$\sigma(k, z) = \frac{1}{2\pi} \int_{-\infty}^{\infty} dx s(x, z) e^{ikx},$$

$$\hat{R}(k) = \frac{1}{2\pi} \int_{-\infty}^{\infty} dx R(x) e^{ikx},$$

Eq. (2.5) is converted to a system of linear equations for ρ and σ :

$$\frac{d}{dz} \begin{pmatrix} \rho \\ \sigma \end{pmatrix} = \begin{pmatrix} 0 & \frac{1}{2}d(z)k^2 \\ -\frac{1}{2}d(z)k^2 + 2g(z)A^2\hat{R} & 0 \end{pmatrix} \begin{pmatrix} \rho \\ \sigma \end{pmatrix}. \quad (2.6)$$

If we were deal with the deterministic system with the parameters d_0 and g_0 , Eq. (2.6) would be the main object to study MI [26]. However, MI induced by the random fluctuations is not captured by the analysis of the first moments $\langle \rho \rangle$ and $\langle \sigma \rangle$ [15], and it is necessary to compute the modulational intensity growth given by the higher-order moments.

III. THE SECOND-ORDER MOMENT MI GAIN

We consider the second moments $\langle \rho^2 \rangle$, $\langle \rho\sigma \rangle$ and $\langle \sigma^2 \rangle$ as constituents of the column vector

$$X^{(2)} = (\langle \rho^2 \rangle, \langle \rho\sigma \rangle, \langle \sigma^2 \rangle)^T. \quad (3.1)$$

The moment $\langle \rho\sigma \rangle$ is added to close the equations for the second-order moments. Then we should calculate z -evolution of the vector $X^{(2)}$. Its first component gives

$$\frac{d}{dz} \langle \rho^2 \rangle = 2\langle \rho_z \rho \rangle = d_0 k^2 \langle \rho\sigma \rangle + d_0 k^2 \langle m_d(z) \rho\sigma \rangle,$$

in accordance with Eqs. (2.2) and (2.6). For decoupling of the mean $\langle m_d(z) \rho\sigma \rangle$ we apply the Furutsu-Novikov formula [28, 29]

$$\langle m_d(z) \rho\sigma \rangle = \int dy \sigma_d^2 B(z-y) \left\langle \frac{\delta}{\delta m_d} \rho\sigma \right\rangle. \quad (3.2)$$

Here $B(z-y) = \delta(z-y)$ for the white-noise Gaussian random process, while the functional derivative $(\delta/\delta m_d)$ is calculated from Eq. (2.6). Indeed, writing $\rho(z)$ as the integral $\rho(z) = (1/2)k^2 \int_0^z dy d(y)\sigma(y)$ (and the similar integral for $\sigma(z)$) and accounting for the explicit representation (2.2) of $d(z)$ in terms of m_d gives

$$\frac{\delta(\rho\sigma)}{\delta m_d} = \frac{\delta\rho}{\delta m_d} \sigma + \rho \frac{\delta\sigma}{\delta m_d} = \frac{1}{2}d_0 k^2 (\sigma^2 - \rho^2).$$

Therefore, $\langle m_d(z) \rho\sigma \rangle = (1/2)\sigma_d^2 d_0 k^2 (\langle \sigma^2 \rangle - \langle \rho^2 \rangle)$ and finally

$$\frac{d}{dz} \langle \rho^2 \rangle = d_0 k^2 \langle \rho\sigma \rangle + \frac{1}{2}\sigma_d^2 d_0^2 k^4 (\langle \sigma^2 \rangle - \langle \rho^2 \rangle).$$

Just in the same way we can calculate z -derivatives of the other components of the vector $X^{(2)}$. As a result, we obtain the evolution equation $(d/dz) X^{(2)} = M^{(2)} X^{(2)}$ with the 3×3 matrix $M^{(2)}$ of the form

$$M^{(2)} = \begin{pmatrix} -\frac{1}{2}\sigma_d^2 d_0^2 k^4 & d_0 k^2 & \frac{1}{2}\sigma_d^2 d_0^2 k^4 \\ 2g_0 A^2 \hat{R} - \frac{1}{2}d_0 k^2 & -\sigma_d^2 d_0^2 k^4 & \frac{1}{2}d_0 k^2 \\ \frac{1}{2}\left(16\sigma_g^2 g_0^2 A^4 \hat{R}^2 + \sigma_d^2 d_0^2 k^4\right) & 2\left(2g_0 A^2 \hat{R} - \frac{1}{2}d_0 k^2\right) & -\frac{1}{2}\sigma_d^2 d_0^2 k^4 \end{pmatrix}. \quad (3.3)$$

Eigenvalues of $M^{(2)}$ with positive real parts lead to instabilities, and the largest positive value determines the MI gain $G_2(k)$. The eigenvalues λ_j are easily found from Eq. (3.3) but they are too cumbersome to be reproduced here explicitly. Below we separately analyze the cases of the defocusing ($g_0 < 0$) and focusing ($g_0 > 0$) nonlinearities. Following [26], we will use for illustration the Gaussian response function

$$R_G(x) = \frac{1}{a\sqrt{\pi}} \exp\left(-\frac{x^2}{a^2}\right), \quad \hat{R}_G(k) = \exp\left(-\frac{1}{4}a^2 k^2\right), \quad (3.4)$$

and the exponential one

$$R_e(x) = \frac{1}{2a} \exp\left(-\frac{|x|}{a}\right), \quad \hat{R}_e(k) = \frac{1}{1+a^2 k^2} \quad (3.5)$$

as examples of the response functions with the sign-definite Fourier images, as well as the rectangular response function

$$R_r(x) = \begin{cases} \frac{1}{2a} & \text{for } |x| \leq a, \\ 0 & \text{for } |x| > a, \end{cases} \quad \hat{R}_r(k) = \frac{\sin(ak)}{ak}, \quad (3.6)$$

whose Fourier transform has negative-sign bands. Here a is the nonlocality parameter, $a \rightarrow 0$ means $R(x) \rightarrow \delta(x)$ and $\hat{R}(k) \rightarrow 1$.

A. Defocusing nonlinearity

For the defocusing nonlinearity $g_0 < 0$ we obtain one real eigenvalue λ_1 and two complex conjugate ones λ_2 and λ_3 . Numerical analysis shows that λ_1 is positive for all k^2 , while λ_2 and λ_3 have negative real parts for the Gaussian and exponential response functions. Let us remind that there is no MI for $g_0 < 0$ for local deterministic Kerr media, while randomness of the coefficients $d(z)$ and $g(z)$ completely destroys stability of the continuous wave solution. This situation considerably changes for nonlocal media. Indeed, Fig. 1 clearly shows that nonlocality with the sign-definite response functions suppresses both the growth rate peak of $G_2(k) \equiv \lambda_1$ and MI bandwidth, the latter being practically finite. When the nonlocality parameter a grows, the suppression effect becomes more pronounced. Somewhat different situation takes place

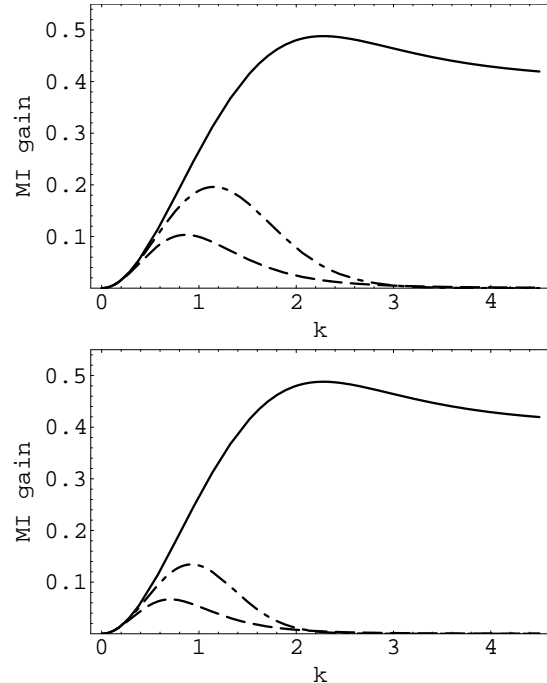


FIG. 1: Defocusing media. Plots of the MI gain $G_2(k)$ for local stochastic medium (solid line), nonlocal stochastic media with the Gaussian (dash-dotted line) and exponential (dashed line) response functions. Here $d_0 = 2$, $|g_0|A^2 = 1$, $\sigma_d^2 = \sigma_g^2 = 0.1$. Upper panel: $a = 1$; lower panel: $a = \sqrt{2}$.

for the rectangular response function (3.6). For sufficiently high nonlocality, MI gain maximum for a given wavenumber k can exceed the corresponding value of G_2 for a local random medium (Fig. 2). Besides, the MI bandwidth becomes strictly finite in this limit.

B. Focusing nonlinearity

In the case of the focusing nonlinearity ($g_0 > 0$) a local deterministic medium produces the long-wave instability with a finite bandwidth. Stochasticity of medium parameters extends the bandwidth to the whole spectrum of modulation wavenumbers. Calculation of eigenvalues of the matrix M_2 (3.3) with $g_0 > 0$ demonstrates that nonlocality suppresses the MI gain and bandwidth for media with both sign-definite (Fig. 3) and sign-indefinite (Fig.

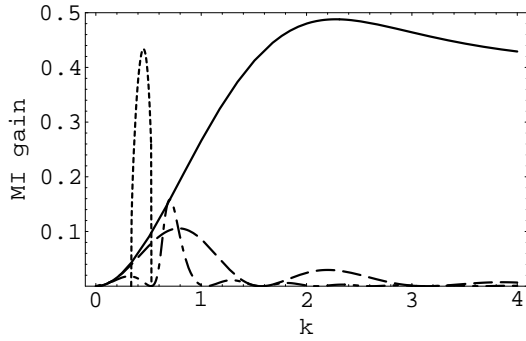


FIG. 2: Defocusing media with the rectangular response function. Plots of the MI gain $G_2(k)$ for local stochastic medium (solid line), nonlocal stochastic media with $a = 2$ (dashed line), $a = 6$ (dash-dotted line), and $a = 10$ (dotted line). Other parameters are the same as in Fig. 1.

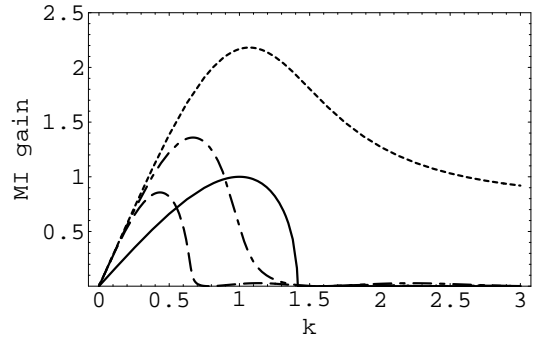


FIG. 4: Focusing media. Plots of the MI gain $G_2(k)$ for a local deterministic medium (solid line), local stochastic medium (dotted line), nonlocal stochastic media with the rectangular response function: $a = 2$ (dash-dotted line), $a = 8$ (dashed line). Other parameters are the same as in Fig. 3.

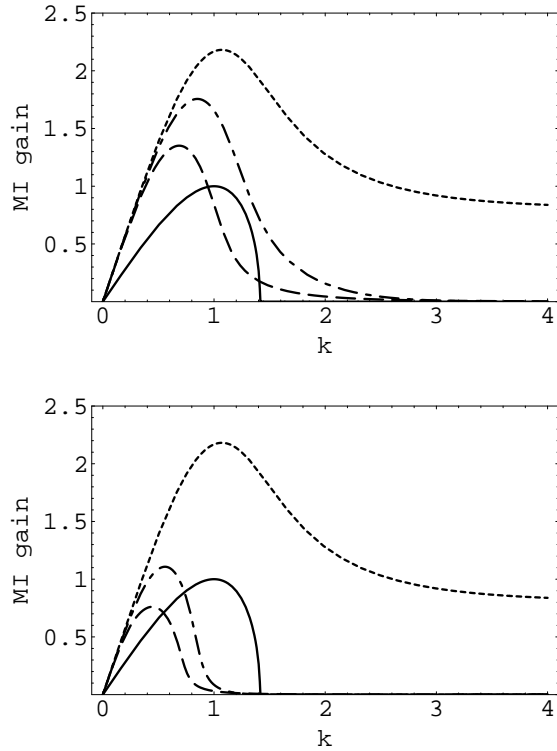


FIG. 3: Focusing media. Plots of the MI gain $G_2(k)$ for a local deterministic medium (solid line), local stochastic medium (dotted line), nonlocal stochastic media with the Gaussian (dash-dotted line) and exponential (dashed line) response functions. Here $d_0 = 2$, $g_0 A^2 = 1$, $\sigma_d^2 = 0.1$, $\sigma_g^2 = 0.2$. Upper panel: $a = 1$; lower panel: $a = 2.5$.

4) response functions. Notice that stronger nonlocality is needed for focusing media to achieve a reduction of the MI gain, as compared with defocusing ones. Besides, maximum positions of the MI gains shift toward smaller wavenumbers k under nonlocality growth, producing finite bandwidth.

IV. HIGHER-ORDER MOMENTS

The second-order moments (3.1) do not provide an analysis of the MI gain in stochastic media with sufficient detail. In particular, it is important to see fluctuations of the exponential growth of the modulation amplitude. More deep insight into the problem demands to account for higher-order moments

$$X^{(2n)} = \left\{ \langle \rho^{(2n-j)} \sigma^j \rangle \right\}, \quad j = 0, \dots, 2n. \quad (4.1)$$

In this section we study the interplay of nonlocality and exponential growth of the higher moments $X^{(2n)}$ in virtue of stochasticity. As before, applying the Furutsu-Novikov formula (3.2), we obtain a matrix $M^{(2n)}$ in the form

$$M^{(2n)} = d_0 k^2 A^{(2n)} + (2g_0 A^2 \hat{R} - \frac{1}{2} d_0 k^2) B^{(2n)} + d_0^2 k^4 \sigma_d^2 C^{(2n)} + 16g_0^2 A^4 \hat{R}^2 \sigma_g^2 D^{(2n)}. \quad (4.2)$$

Non-zero entries of the matrices $A^{(2n)}$, $B^{(2n)}$, $C^{(2n)}$ and $D^{(2n)}$ are written as

$$A_{j,j+1}^{(2n)} = n - \frac{j}{2}, \quad B_{j,j-1}^{(2n)} = j; \quad C_{jj}^{(2n)} = -\frac{1}{2}(n+2nj-j^2),$$

$$C_{j,j+2}^{(2n)} = \left(n - \frac{j}{2} \right) \left(n - \frac{j+1}{2} \right), \quad (4.3)$$

$$C_{j,j-2}^{(2n)} = D_{j,j-2}^{(2n)} = \frac{1}{4} j(j-1), \quad j = 0, \dots, 2n.$$

Then the maximal real part of roots of the characteristic polynomial $\det |M^{(2n)} - \lambda I|$ will give $nG_{2n}(k)$. Since all the matrix elements of $M^{(2n)}$ are real and the characteristic polynomial is of the odd degree, at least one of the eigenvalues of $M^{(2n)}$ is real and the others are mutually complex conjugate. In what follows we will consider the 4-th and 6-th moments.

A. Defocusing nonlinearity

In Fig. 5 we show the results of calculating MI gains G_2 , G_4 and G_6 for both the exponential and Gaussian response functions and compare them with the same curves for local stochastic media obtained in [15]. It is seen that nonlocality suppresses the higher-order moments as well. Notice that in defocusing media positions of MI gain maxima for moments of different orders coincide [15] (they are deterministic rather than random). Nonlocality does not disturb this property. Fig. 6 demonstrate similar curves for the rectangular response function for different values of the nonlocality parameter a . It is seen that for sufficiently high a the medium demonstrates practically coinciding distributions of higher-moment growth rates, their maxima being shifted to shorter wavelengths. Evidently, higher-order moments for the rectangular response function manifest the same “anomalous” enhancement of the growth rate in a narrow region of modulation wavenumbers, as compared with the local stochastic case.

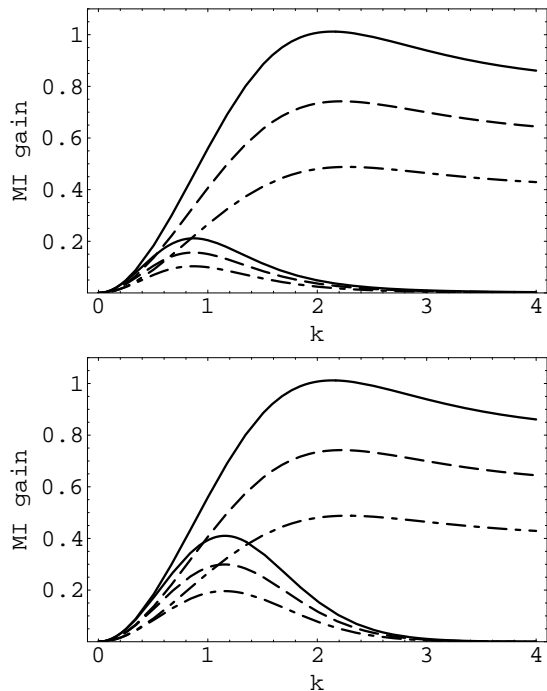


FIG. 5: Defocusing media. Plots of the MI gains G_6 (solid line), G_4 (dashed line), and G_2 (dash-dotted line) for a local stochastic medium (upper three curves) and for nonlocal stochastic media (lower three curves). Here $d_0 = 2$, $a^2 = 1$, $|g_0|A^2 = 1$, $\sigma_a^2 = \sigma_g^2 = 0.1$. Upper panel: exponential response function; lower panel: Gaussian response function.

B. Focusing nonlinearity

For the focusing media the higher-order MI gains demonstrate much the same behavior as for the defocusing ones for both sign-definite and sign-indefinite re-

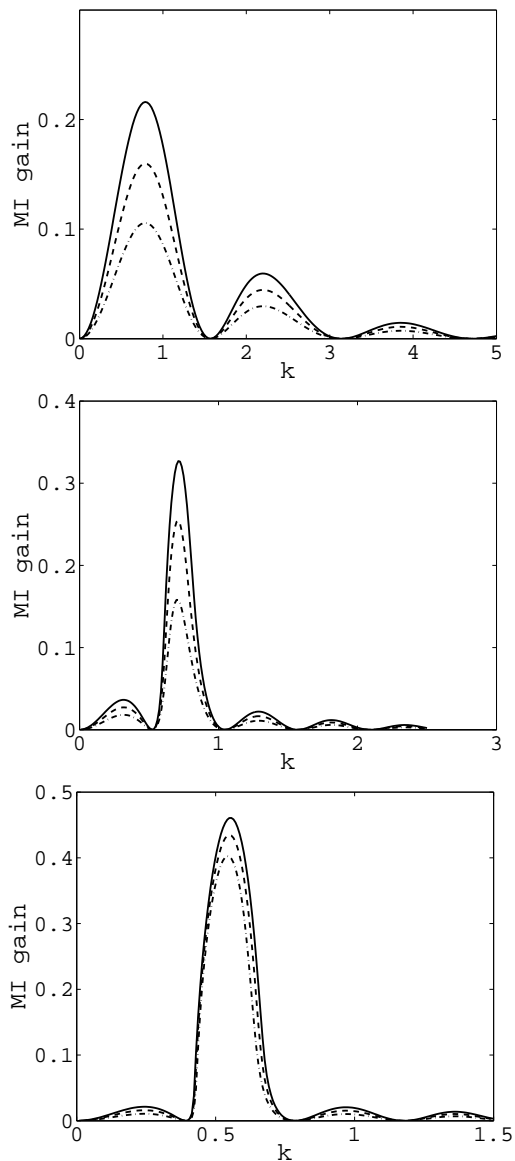


FIG. 6: Defocusing nonlocal stochastic media with the rectangular response function. Plots of the MI gains G_6 (solid line), G_4 (dashed line), and G_2 (dash-dotted line) for $d_0 = 2$, $|g_0|A^2 = 1$, $\sigma_a^2 = \sigma_g^2 = 0.1$. Upper panel: $a = 2$; middle panel: $a = 6$; lower panel: $a = 8$.

sponse functions. Fig. 7 shows the MI gains for local and nonlocal stochastic media for the Gaussian response function. Curves for the exponential and rectangular response functions are qualitatively the same. With increasing the nonlocality parameter a , curves for MI gains of different orders become closer one the other, so high nonlocality smoothes fluctuations of the modulation amplitude growth.

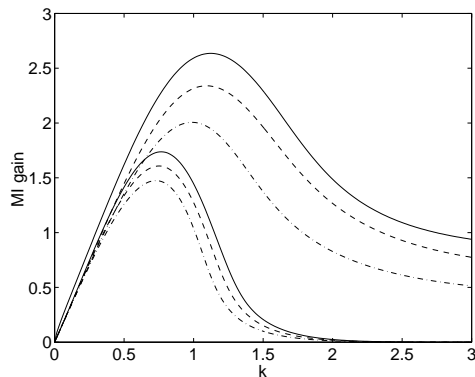


FIG. 7: Focusing media. Plots of the MI gains G_6 (solid line), G_4 (dashed line), and G_2 (dash-dotted line) for a local stochastic medium (upper three curves) and for nonlocal stochastic medium with the Gaussian response function (lower three curves). Here $d_0 = 2$, $a = 2$, $g_0 A^2 = 1$, $\sigma_d^2 = \sigma_g^2 = 0.1$.

V. CONCLUSION

Within the limits of the linear stability analysis, we have investigated the MI of a homogeneous wave in a

nonlocal nonlinear Kerr-type medium with random parameters. For the case of the white-noise model of parameter fluctuations, we derived the equations which govern the dependence of the MI gain on the modulation wavenumber. As was expected from physical motivations, nonlocality causes considerable suppression of the stochasticity-induced MI growth rate for media with the sign-definite Fourier images of the response functions. At the same time, nonlocal media with the sign-indefinite Fourier images of the response functions can display a somewhat different behavior leading to an increase, as compared with local media, of the MI gain for some domains of modulation wavenumbers.

Acknowledgments

The authors are very grateful to F. Abdullaev and J. Garnier for constructive comments.

-
- [1] G.A. Askar'yan, Zh. Eksp. Teor. Fiz. **42**, 1576 (1962) [Sov. Phys. JETP **15**, 1088 (1962)].
 - [2] T. Taniuti and H. Washini, Phys. Rev. Lett. **21**, 209 (1968).
 - [3] V.I. Bespalov and V.I. Talanov, Pis'ma Zh. Eksp. Teor. Fiz. **3**, 471 (1966) [JETP Lett. **3**, 307 (1966)].
 - [4] L.A. Ostrovskii, Zh. Eksp. Teor. Fiz. **51**, 1189 (1966) [Sov. Phys. JETP **24**, 797 (1967)].
 - [5] T.B. Benjamin and J.E. Feir, J. Fluid Mech. **27**, 417 (1967).
 - [6] B. Wu and Q. Niu, Phys. Rev. A **64**, 061603 (2001).
 - [7] V.V. Konotop and M. Salerno, Phys. Rev. A **65**, 021602(R) (2001).
 - [8] L. Salasnich, A. Parola, and L. Reatto, Phys. Rev. Lett. **91**, 080405 (2003).
 - [9] K. Tai, A. Hasegawa, and A. Tomita, Phys. Rev. Lett. **56**, 135 (1986).
 - [10] G. Millot, E. Seve, S. Wabnitz, and M. Haelterman, J. Opt. Soc. Am. B **15**, 1266 (1998).
 - [11] K.E. Stecker, G.B. Partridge, A.G. Truscott, and R.J. Hulet, Nature **417**, 150 (2002).
 - [12] Yu.S. Kivshar and G.P. Agrawal, *Optical Solitons: From Fibers to Photonic Crystals*, Academic Press, San Diego, 2003.
 - [13] F.Kh. Abdullaev, S.A. Darmanyan, S. Bishoff, and H.P. Sørensen, J. Opt. Soc. Am. B **14**, 27 (1997).
 - [14] M. Karlsson, J. Opt. Soc. Am. B **15**, 2269 (1998).
 - [15] J. Garnier and F.Kh. Abdullaev, Physica D **145**, 65 (2000).
 - [16] F.Kh. Abdullaev, S.A. Darmanyan, and J. Garnier, Progr. Opt. **44**, 303 (2002).
 - [17] A. Dreischuh, G.G. Paulus, F. Zacher, F. Grasbon, and H. Walther, Phys. Rev. E **60**, 6111 (1999).
 - [18] D. Suter and T. Blasberg, Phys. Rev. A **48**, 4583 (1993).
 - [19] C. Conti, M. Peccianti, and G. Assanto, Phys. Rev. Lett. **91**, 073901 (1993); **92**, 113902 (2004).
 - [20] M. Segev, B. Crosignani, A. Yariv, and B. Fischer, Phys. Rev. Lett. **68**, 923 (1992).
 - [21] G.C. Duree, J.L. Shultz, G.J. Salamo, M. Segev, A. Yariv, B. Crosignani, P. Di Porto, E.J. Sharp, and R.R. Neurgaonkar, Phys. Rev. Lett. **71**, 533 (1993).
 - [22] V.M. Perez-Garcia, V.V. Konotop, and J.J. Garcia-Ripoll, Phys. Rev. E **62**, 4300 (2000).
 - [23] S.K. Turitsyn, Teor. Mat. Fiz. **64**, 226 (1985) [Theor. Math. Phys. **64** 797 (1985)].
 - [24] O. Bang, W. Krolikowski, J. Wyller, and J.J. Rasmussen, Phys. Rev. E **66**, 046619 (2002).
 - [25] A. Dreischuh, D. Neshev, D.E. Peterson, O. Bang, and W. Krolikowski, Phys. Rev. Lett. **96**, 043901 (2006).
 - [26] W. Krolikowski, O. Bang, J.J. Rasmussen, and J. Wyller, Phys. Rev. E **64**, 016612 (2001).
 - [27] W. Krolikowski, O. Bang, N.J. Nikolov, D.N. Neshev, J.J. Rasmussen, J. Wyller, and D. Edmundson, J. Opt. B: Quantum Semiclass. Opt. **6**, S288 (2004).
 - [28] K. Furutsu, J. Res. NBS, **D-67**, 303 (1983).
 - [29] E.A. Novikov, Sov. Phys. JETP **20**, 1290 (1964).